

Contact atomic structure and electron transport through molecules

San-Huang Ke

Department of Chemistry, Duke University, Durham, North Carolina 27708-0354 and Department of Physics, Duke University, Durham, North Carolina 27708-0305

Harold U. Baranger

Department of Physics, Duke University, Durham, North Carolina 27708-0305

Weitao Yang

Department of Chemistry, Duke University, Durham, North Carolina 27708-0354

(Received 3 August 2004; accepted 2 December 2004; published online 11 February 2005)

Using benzene sandwiched between two Au leads as a model system, we investigate from first principles the change in molecular conductance caused by different atomic structures around the metal-molecule contact. Our motivation is the variable situations that may arise in break junction experiments; our approach is a combined density functional theory and Green function technique. We focus on effects caused by (1) the presence of an additional Au atom at the contact and (2) possible changes in the molecule-lead separation. The effects of contact atomic relaxation and two different lead orientations are fully considered. We find that the presence of an additional Au atom at each of the two contacts will increase the equilibrium conductance by up to two orders of magnitude regardless of either the lead orientation or different group-VI anchoring atoms. This is due to a resonance peak near the Fermi energy from the lowest energy unoccupied molecular orbital. In the nonequilibrium properties, the resonance peak manifests itself in a negative differential conductance. We find that the dependence of the equilibrium conductance on the molecule-lead separation can be quite subtle: either very weak or very strong depending on the separation regime. © 2005 American Institute of Physics. [DOI: 10.1063/1.1851496]

I. INTRODUCTION

Understanding electron transport through nanoscale junctions or molecular devices connected to metallic electrodes may be the basis of future molecular electronics technology.¹⁻⁵ One of the critical issues in this regard is to construct contact structures which can provide both useful stability and high contact transparency.

In many recent experiments,^{3,6-8} Au electrodes were used as leads for transport measurements because of the high conductivity, stability, and well-defined fabrication techniques involved. A common way to construct a lead-molecule-lead (LML) system is by using a break junction. These can be made either through electromigration⁹⁻¹² or through direct mechanical means^{6-8,13} [i.e., mechanically controllable break junction (MCBJ)]. In these break-junction experiments the detailed atomic structure of the molecule-lead contacts of a LML system is unknown. In fact, because of the atomic scale roughness of the break surface, different atomic scale structures of the contact may occur in different experiments. Up to now, it has been difficult to investigate and control experimentally the detailed contact atomic structure and find out its influence on the electron transport through a molecular device. Here theoretical modeling/simulation free from empirical parameters may play an important role in understanding, interpreting observed experimental behaviors, or doing predesigned for good contact structures.

Because of the need for an atomic scale description, *ab initio* density functional theory (DFT) (Refs. 14 and 15) is a

natural approach to molecular electronics. One route works explicitly with scattering states via the Lippmann-Schwinger equation.¹⁶⁻¹⁹ The more common method, however, is to combine DFT using a localized basis set for molecular electronic structure with the nonequilibrium Green function method (NEGF) (Refs. 20 and 21) for electron transport.²²⁻²⁷ In this method some parts of the electrodes of a LML system can be included in the device region to form an “extended molecule,” and therefore the specific contact atomic structure and relaxation can be fully considered in principle although in practice the atomic structure is usually predetermined to avoid the heavy computational effort.²⁸⁻⁴⁰ In the implementations of this approach, some researchers^{23,24,26,28-32} adopted quantum chemistry methods for the DFT calculation in which a cluster geometry is used for the device region, while others^{22,25,27,33-40} used a periodic geometry (as in solid state physics) for the device region. The advantages of the latter are that the electronic structure of the device region and the two leads can be easily treated on the same footing and the infinite LML system is nearly perfect in geometry without any artificially introduced surface effect and scattering.

Previously we developed a self-consistent approach within the DFT+NEGF method for calculating electron transport through molecular devices.²⁷ Our approach is simple while strict: the nonequilibrium condition under a bias is fully included in the NEGF rather than the DFT part. Therefore, it is straightforward to combine with any electronic structure method that uses a localized basis set. More importantly, in this way we avoid the problem of solving for

the Hartree potential under a bias field with unphysical potential jumps at the two boundaries of the DFT supercell. In our method large parts of the two metallic leads of a system are included in the device region so that the molecule-lead interactions (including electron transfer and atomic relaxation) are fully included, and the electronic structures of the molecule and the two leads are treated exactly on the same footing.

Based on this method, here we report an investigation of the molecular conductance of benzene connected to two Au leads with finite cross section. At each step, the reasonability of the present systematic results are discussed in comparison with the prior results from Xue and Ratner^{29,30} for an unrelaxed S-anchored Au(111) system and from Di Ventra, *et al.*^{18,41} who used a jellium model. We focus on the effects of changing the atomic structure around the contacts, including the presence of an additional Au atom and changes in the molecule-lead separation, both of which are simple but important situations in break-junction experiments. In our calculation the effects of contact atomic relaxation and different lead orientations are fully considered. Also considered are different group-VI anchoring atoms. Our calculations show a dramatic effect of contact atomic configuration on electron transport through the molecule: an additional Au atom at the contacts can increase the equilibrium conductance by two orders of magnitude due to a resonance peak around the Fermi energy from the lowest energy unoccupied molecular orbital (LUMO). We find that the dependence of the equilibrium conductance on the molecule-lead separation can be complicated: either very weak or very strong depending on the separation regime.

II. SYSTEMS INVESTIGATED AND COMPUTATIONAL DETAILS

The systems we have studied consist of a benzene molecule connected to two Au leads of finite cross-section through a S atom located at the hollow site of the Au(001) or Au(111) surface. While the use of leads with a finite cross section is more efficient in our method it is an approximation to real experimental situations. In MCB technique a metal wire is elongated and broken by the bending of the substrate. Experiments^{13,42} have shown that well before a metal wire breaks a very thin bridge region is formed which contributes only several G_0 ($=2e^2/h$, conductance quantum) of conductance to the wire. This means that in a real LML system the molecule is usually connected to a very thin nanowire which is then connected to the extended part of the metal lead. Therefore the real experimental situation is between the following two limits: a lead of thin nanowire and a lead of infinitely wide surface. In this paper we adopt the former limit and the width of the Au leads is set to be $2\sqrt{2} \times 2\sqrt{2}$ for the (001) lead and 2×2 for the (111) lead. To see the possible effect of the small width on the results we also carry out calculations using wider leads: $3\sqrt{2} \times 3\sqrt{2}$ and $4\sqrt{2} \times 4\sqrt{2}$ for (001), 3×3 and 4×4 for (111).

To investigate the role of contact atomic structure, here we consider a very simple but possible situation: the presence of an additional Au atom at either one or both contacts,

denoted by 1Au and 2Au, respectively. We use the structural label (001)_1Au, for instance, to denote the system with the Au(001) leads and an additional Au atom at one of its contacts. To show the effect of change in the molecule-lead separation, we change rigidly (i.e., without any further structure relaxation) the contact Au–S distance ($d_{\text{Au-S}}$) in the vertical direction. The purpose of all these considerations is to simulate possible situations in break-junction experiments in which different contact atomic structures may occur because of atomic fluctuations on the break surfaces and the molecule-lead separation can be adjusted by the MCB technique. To show the effect of contact atomic relaxation, we calculate the electron transmission for two independent cases: (1) Atoms in the leads are fixed at their bulk positions, and the molecule is fixed at the optimized structure of the isolated molecule with the dangling bond on the S atom saturated by an Au atom. The distance between the S atom and the Au surface, however, is optimized. This structure is called “unrelaxed.” (2) The structure of the molecule, the first two atomic layers of the lead surfaces, as well as the molecule-lead separation are fully relaxed. The in-plane position of the S atom is, however, fixed at the hollow site. This structure is called “relaxed;” the structure of the relaxed systems are shown in Fig. 1.

We use the efficient full DFT package SIESTA (Ref. 43) to do the electronic structure calculation. It adopts a finite-range numerical basis set and makes use of pseudopotentials for the atomic cores. We adopt a high level double ζ plus polarization (DZP) basis set for all atomic species. The PBE version of the generalized gradient approximation (Ref. 44) is adopted for the electron exchange and correlation, and optimized Troullier–Martins pseudopotentials (Ref. 45) are used for the atomic cores. The atomic structure of the relaxed systems are optimized until the maximum residual force on all atoms is less than $0.02 \text{ eV}/\text{\AA}$.

For the transport calculation, we divide an infinite LML system into three parts: left lead L , right lead R , and device region C which contains the molecule and large parts of the left and right leads, as shown in Fig. 1, so that the molecule-lead interactions can be fully accommodated. Under a bias V_b the region C will be driven out of equilibrium. We have developed a simple while strict full self-consistent approach²⁷ to handle a steady state bias: The bias is included through the density matrix of the region C (\mathbf{D}_C) in the Green function calculation instead of the potential (\mathbf{H}_C) in the DFT part. Specifically, we calculate \mathbf{D}_C under the boundary condition that there is a potential difference V_b between the left side of region C (together with the left lead) and the right side of C (together with the right lead),

$$\mathbf{D}_C = \frac{1}{2\pi} \int_{-\infty}^{+\infty} dE \left[\mathbf{G}_C(E) \Gamma_L \left(E + \frac{eV_b}{2} \right) \mathbf{G}_C^\dagger(E) f(E - \mu_L) + \mathbf{G}_C(E) \Gamma_R \left(E - \frac{eV_b}{2} \right) \mathbf{G}_C^\dagger(E) f(E - \mu_R) \right], \quad (1)$$

where $\mathbf{G}_C(E)$ is the retarded Green function of region C (in which all the potential shifts are included²⁷), f is the Fermi function, and μ_L and μ_R the chemical potentials of the leads. $\Gamma_L(E)$ and $\Gamma_R(E)$ reflect the coupling at energy E between

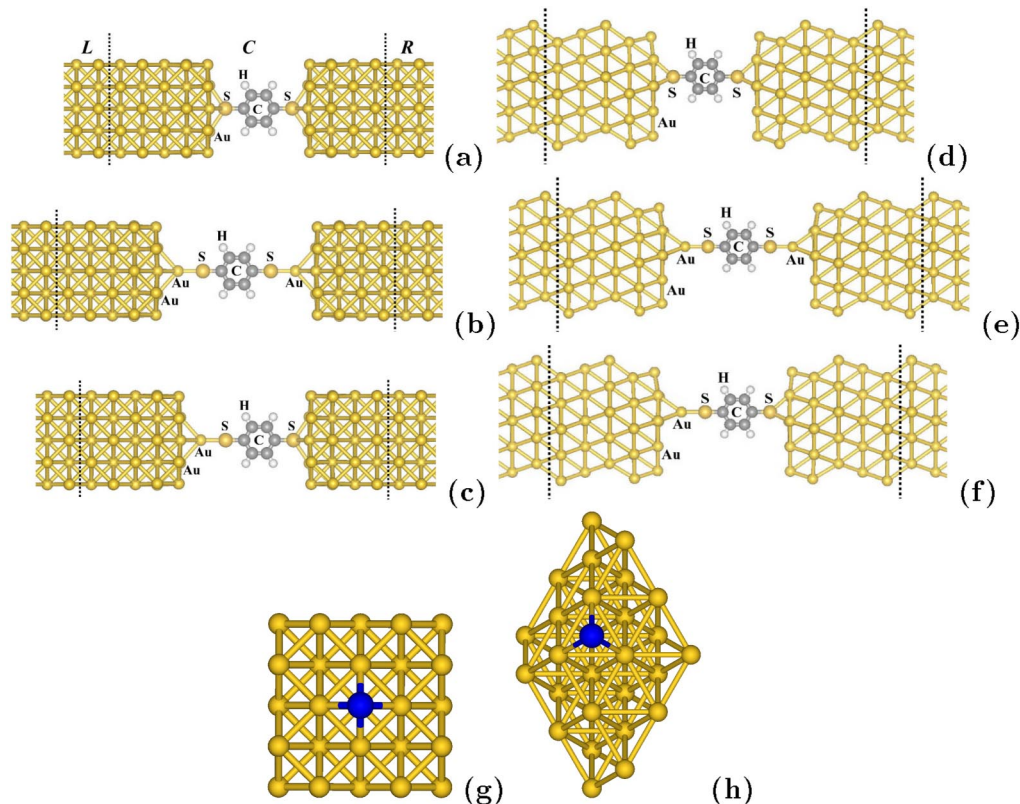


FIG. 1. Optimized atomic structures of the LML systems investigated, obtained by relaxing fully the molecule, the first two atomic layers of the two lead surfaces, and the molecule-lead separation. (a), (b), and (c): The Au leads are in the (001) direction, and there are 0, 2, and 1 additional Au atoms at the contacts, respectively. (d), (e), and (f): The Au leads are in (111) direction, and there are 0, 2, and 1 additional Au atoms at the contacts, respectively. The dashed line indicates the interface between the device region (C) and the left or right lead (L or R). The in-plane adsorption site of the molecule is indicated by a dark-colored ball in (g) for (001) and in (h) for (111).

the C region and the leads L and R. The self-consistent loop is $\rightarrow \mathbf{H}_C(\text{DFT}) \rightarrow \mathbf{G}_C \rightarrow \mathbf{D}_C(\text{NEGF}) \rightarrow \mathbf{H}_C(\text{DFT}) \rightarrow \dots$ until \mathbf{H}_C and \mathbf{D}_C converge.²⁷ The electron transmission through C is then related to Green functions by

$$T(E, V_b) = \text{Tr} \left[\Gamma_L \left(E + \frac{eV_b}{2} \right) \mathbf{G}_C(E) \Gamma_R \left(E - \frac{eV_b}{2} \right) \mathbf{G}_C^\dagger(E) \right]. \quad (2)$$

Note how V_b again appears in Γ here. Finally, the steady-state current is obtained by simply integrating the transmission over the energy window.

III. RESULTS AND DISCUSSION

A. Equilibrium transmission and electron transfer

In Fig. 2 we show the transmission functions for both the unrelaxed and the relaxed systems. The calculated values of equilibrium conductance are given in Table I, together with the molecule-lead electron transfer determined by a Mulliken population analysis (a positive value means electrons are transferred from the Au leads to the molecule, including the two S atoms).

Because we use the bulk Au structure for the leads in the unrelaxed cases, the contact atomic relaxation consists of two parts: (1) the relaxation of the bare Au lead with respect to its bulk structure, and (2) the relaxation of both the leads and the molecule induced by the molecule-lead interaction.

Our calculations of optimized atomic structure show that both parts are very small, as can be seen in Fig. 1. The small relaxation of the bare Au leads is consistent with the very small surface relaxation of unreconstructed infinite Au surfaces. The small molecule-lead relaxation is understandable because the hollow site corresponds to a bulk atomic position, and so the absorption of a S atom will not markedly change the directional binding of the surface. Because the contact atomic relaxation is very small, its effect on electron transmission is only minor: as seen in Fig. 2 and Table I, the induced change in equilibrium conductance is less than 100%. The very small molecule-lead relaxation justifies the reasonability of changing rigidly $d_{\text{Au-S}}$ for simulating the change in the molecule-lead separation.

The results in Table I show that if there is no additional Au atom at the contacts (0Au systems), the Au(001) lead yields a larger conductance than Au(111). This may be understood by considering the contact atomic configuration in the two cases: the S atom touches four Au atoms on the Au(001) surface [see Fig. 1(g)] but only three on Au(111) [see Fig. 1(h)]. Note that this difference in conductance is significantly reduced by adding additional Au atoms to the contacts. This is obvious according to the above analysis: the additional Au atom reduces the structural difference for electron transport between the Au(001) and Au(111) contacts. Another difference between the two lead orientations is in the overall structure of $T(E)$, as shown in Fig. 2: The $T(E)$

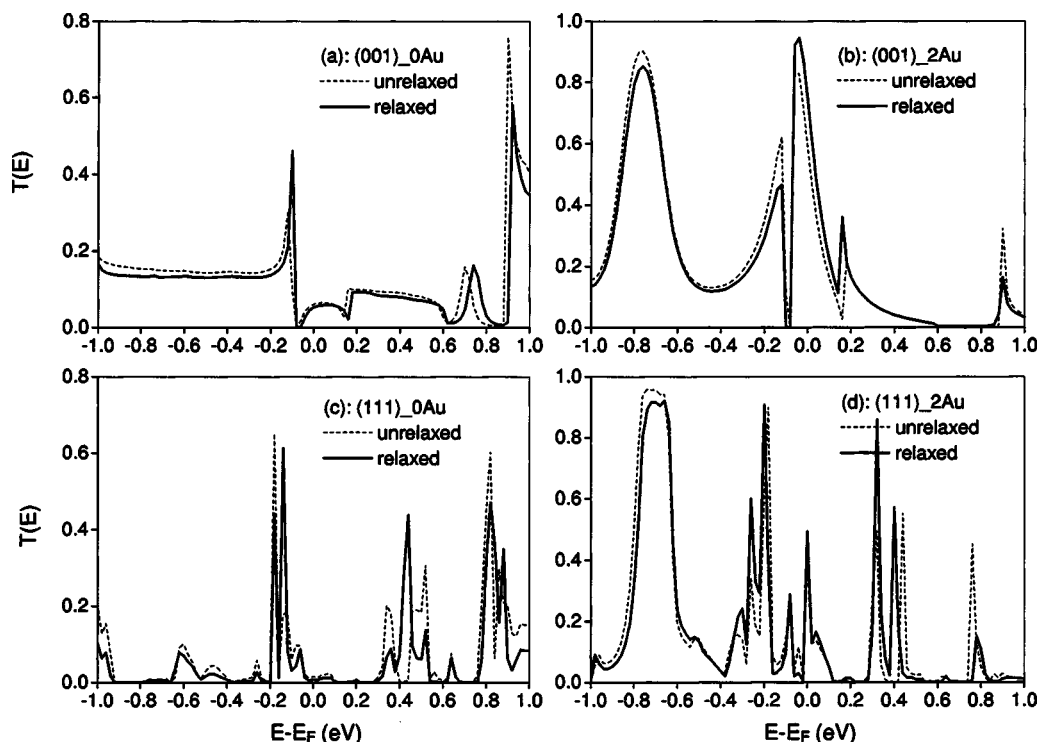


FIG. 2. Comparison between the transmission functions of the unrelaxed (dashed line) and the relaxed (solid line) systems. Different systems are indicated by their structure labels as defined in the text. (a), (b), (c), and (d) correspond to the atomic structures of (a), (b), (d), (e) in Fig. 1, respectively.

functions of the Au(111) systems have more sharp structures than those of the Au(001) systems. This difference is related to the thinner Au(111) lead and its much lower symmetry. This behavior of the Au(111) lead has also been found in other calculations.²⁵

The introduction of Au atoms to the contacts causes a dramatic change in the conductance of the system. The calculated values of equilibrium conductance in Table I show that an additional Au atom at both contacts increases the conductance by a factor of 14 for the Au(001) lead and 61 for Au(111). From the calculated transmission functions in Fig. 2, we see clearly that the two additional Au atoms produce a large resonance around the Fermi energy. It will be shown later that this originates from the LUMO level of the isolated molecule (i.e., S-C₆H₄-S). The driving forces causing the resonance peak are the molecule-lead electron transfer and coupling. As seen in Table I, the introduction of the two

additional Au atoms changes the sign of the electron transfer so that more electrons are transferred from the leads to the molecule, finally causing the (broadened) molecular LUMO level to line up with the chemical potential of the leads. This point will be confirmed directly later. To show more clearly the difference between the systems with and without the additional Au atoms we show in Fig. 3 the local density of states within the energy window $[-0.05, +0.05]$ around the Fermi energy for the systems (001)_0Au and (001)_2Au. The two additional Au atoms clearly lead to a conductance channel in the (001)_2Au system which is absent in the (001)_0Au case. Note that the spatial shape of the density of states on the molecule indicates that the channel is formed from the LUMO level. When we add the Au to only one of the two contacts [see the atomic structures in Fig. 1(e) and 1(f)], the increase in conductance is only minor (see the rows with label “1Au” in Table I), especially for the Au(001) lead, indicating that the electron transmission through the molecule is then choked off by the less transparent contact.

In order to check possible influences of the small lead width on these results, we carried out further calculations using the following wider leads: $3\sqrt{2} \times 3\sqrt{2}$ and $4\sqrt{2} \times 4\sqrt{2}$ for (001), 3×3 and 4×4 for (111). Here we adopted the unrelaxed structures as described previously and a smaller basis set, single ζ plus polarization (SZP), to reduce the much larger computational effort. The results are listed in Table II. To have a consistent comparison, in Table II we also list the results from the small-basis-set calculation for the small leads. As can be seen, the basis set effect is quite small except for the (001)_2Au system, for which the DZP basis set gives a conductance two times larger than the SZP result. For the same basis set (i.e., SZP) the wider leads give quantita-

TABLE I. Calculated equilibrium conductance (G , in units of $2e^2/h$) and molecule-lead electron transfer (ΔQ , in units of electron, a positive value means that electrons are transferred from lead to molecule). Note the large effect of adding additional Au atoms.

			Unrelaxed		Relaxed	
			ΔQ	G	ΔQ	G
S	(001)	0Au	-0.026	0.061	-0.048	0.053
		1Au			+0.169	0.059
		2Au	+0.200	0.590	+0.261	0.740
	(111)	0Au	+0.044	0.016	+0.053	0.0080
		1Au			+0.204	0.025
		2Au	+0.178	0.380	+0.228	0.490

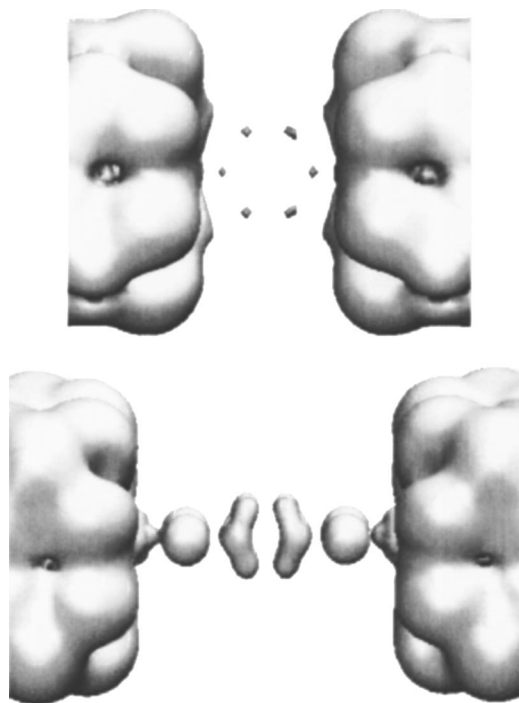


FIG. 3. Local density of states within the energy window (-0.05 , $+0.05$) eV around the Fermi energy for the systems (001)₀Au (upper) and (001)₂Au (lower). Note the channel with LUMO-like character in the latter which is absent in the former.

tively somewhat different results from the thinner leads, but the conclusion concerning the significant role of the additional Au atoms remains the same.

B. Other anchoring atoms

In order to examine whether this behavior is common for other group-VI anchoring atoms, we carry out the same calculation for systems having similar geometry but anchored by Se and Te atoms. The results of equilibrium conductance and molecule-lead electron transfer are listed in Table III. Clearly, the conclusions reached in the S-anchored systems also holds for the Se- and Te-anchored systems.

C. Dependence on molecule-lead separation

In MCB experiments the molecule-lead separation may not be at its equilibrium value but rather may be lengthened or compressed because of the mismatch between the molecular length and the junction break. To simulate this situation,

TABLE II. Equilibrium conductance (in units of $2e^2/h$) calculated by using the wider leads and the smaller basis set as mentioned in the text. For a consistent comparison, we also list the results from the small-basis-set calculation for the small leads. Note the same effect of adding additional Au atoms, as shown in Table I.

S	(001)	$2\sqrt{2} \times 2\sqrt{2}$	$3\sqrt{2} \times 3\sqrt{2}$	$4\sqrt{2} \times 4\sqrt{2}$
	0Au	0.072	0.090	0.089
	2Au	0.273	0.255	0.260
	(111)	2×2	3×3	4×4
	0Au	0.017	0.010	0.057
	2Au	0.292	0.470	0.581

TABLE III. Calculated equilibrium conductance (G , in units of $2e^2/h$) and molecule-lead electron transfer (ΔQ , in units of electron) for the Se- and Te-anchored systems. (The notations are the same as those in Table I). All the trends seen in the S anchored systems are also evident here.

			Unrelaxed		Relaxed	
			ΔQ	G	ΔQ	G
Se	(001)	0Au	-0.190	0.036	-0.206	0.031
		1Au			+0.099	0.044
		2Au	+0.220	0.490	+0.283	0.660
	(111)	0Au	-0.042	0.010	-0.010	0.0047
		1Au			+0.167	0.036
		2Au	+0.198	0.357	+0.235	0.550
Te	(001)	0Au	-0.318	0.017	-0.294	0.014
		1Au			+0.052	0.024
		2Au	+0.228	0.260	+0.290	0.420
	(111)	0Au	-0.088	0.0050	-0.044	0.0024
		1Au			+0.155	0.022
		2Au	+0.216	0.240	+0.261	0.430

here we calculate the equilibrium conductance as a function of the change in $d_{\text{Au-S}}$ ($\Delta d_{\text{Au-S}}$) with regard to its equilibrium value for three systems: unrelaxed (001)₂Au, (001)₀Au, and relaxed (001)₁Au. For the first two cases, $d_{\text{Au-S}}$ of both contacts will be changed rigidly while maintaining the symmetry of the system, while for the third case only $d_{\text{Au-S}}$ of the contact without the additional Au atom will be changed rigidly. As mentioned previously, the very small molecule-lead relaxation justifies this treatment. The results are shown in Fig. 4.

There is a large resonance peak in the conductance curve for all three systems. For the (001)₂Au case, the equilibrium Au-S distance is very close to the position of the resonance peak, while for the other two systems the equilibrium Au-S distance is about 1.4 Å away from the position of the resonance peak. Along with the increase of $\Delta d_{\text{Au-S}}$ the amount of charge transferred from the leads to the molecule increases and reach its maximum around the resonance peak. If we assume the mechanism producing the resonance is the same for the three systems, then $T(E)$ at point C in Fig. 4(b) should be similar to that at point A in Fig. 4(a), even though transmission at points A and B are very different [see Fig. 2(b) and 2(a)]. To check our point we plot the transmission function for point C in Fig. 4(d). It is clear that, as expected, this $T(E)$ is quite similar to that of Fig. 2(b).

Before continuing to investigate the mechanism of the resonance, we briefly pause to compare to previous calculations available for the S-anchored system. In Refs. 29 and 30, Xue and Ratner reported on a systematic calculation for the unrelaxed S₍₁₁₁₎_h system adopting a cluster method in which six Au atoms of each lead surface are included to form the extended molecule. They found that an additional Au atom introduced at each contact will increase significantly the equilibrium conductance and that this effect is quite similar to that from increasing the contact Au-S distance. Although there are some quantitative differences between the two sets of results, our results are consistent with their findings despite the fact that the techniques adopted in

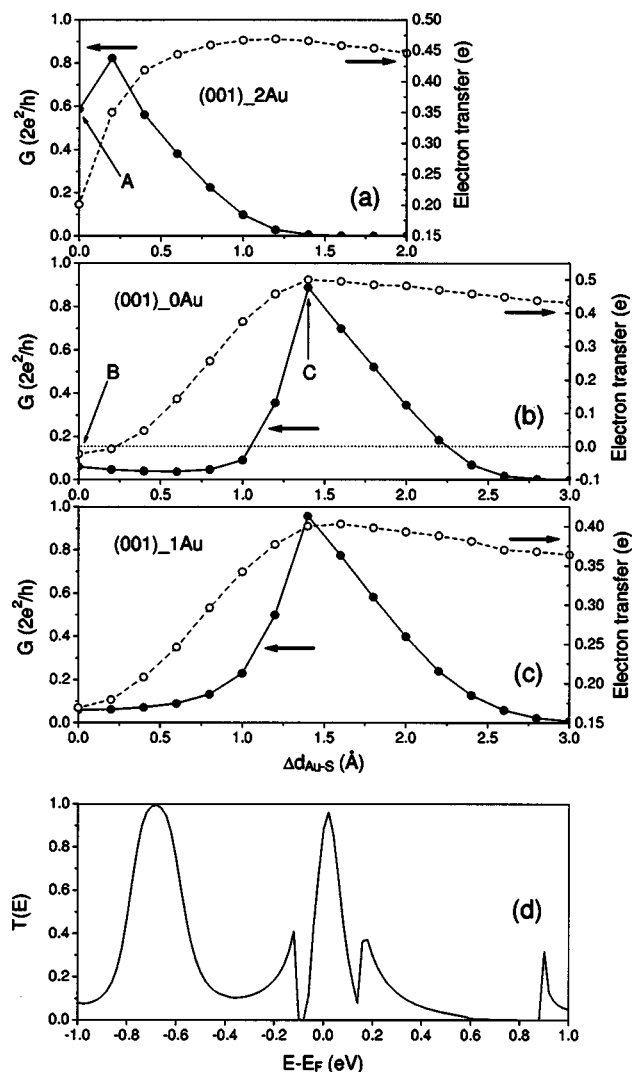


FIG. 4. Equilibrium conductance and lead-to-molecule electron transfer as functions of the change in Au-S distance ($\Delta d_{\text{Au-S}}$), for (a) unrelaxed (001)₂Au system, (b) unrelaxed (001)₀Au system, and (c) relaxed (001)₁Au system. In (a) and (b) $d_{\text{Au-S}}$ of the two contacts is rigidly and symmetrically changed, while in (c) only $d_{\text{Au-S}}$ of the contact without the additional Au is rigidly changed. The transmission function for point C is shown in (d), while those for points A and B are already shown in Figs. 2(b) and 2(a), respectively. Note the large resonance conductance peak in panels (a)–(c) accompanied by significant electron transfer to the molecule. The similarity of (d) to Fig. 2(b) shows that increased Au-S separation has an effect comparable to that of the extra Au atoms.

the two calculations are very different: (1) In our calculation both the lead and molecule are treated by DFT (Ref. 46) while in Refs. 29 and 30 the molecule is treated by DFT but the lead is treated by a tight-binding approach. (2) Periodic boundary conditions for DFT are used here with large parts of the leads (more than 45 Au atoms in each lead) included into the device region⁴⁷ while the cluster geometry is used in Refs. 29 and 30. On the other hand, in Ref. 41 Ventra, Lang, and Pantelides reported a systematic calculation of the conductance of the 1,4-dithiol-benzene molecule by using a jellium model for the Au lead. They found that the introduction of an additional Au atom at each contact will decrease significantly the equilibrium conductance. Although their calculation also shows the strong contact structure dependence of the molecular conductance, the result is qualitatively differ-

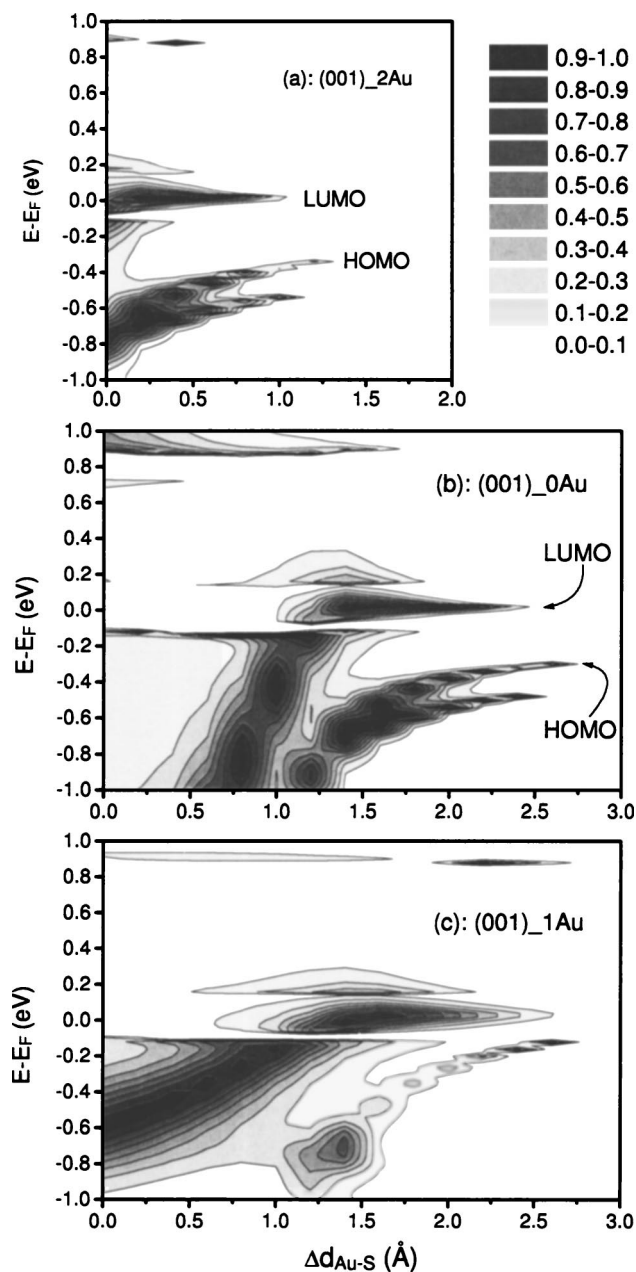


FIG. 5. Contour plots of transmission as a function of both energy and $\Delta d_{\text{Au-S}}$ for (a) unrelaxed (001)₂Au system, (b) unrelaxed (001)₀Au system, and (c) relaxed (001)₁Au system. The meaning of $\Delta d_{\text{Au-S}}$ is the same as in Fig. 4. The contributions from the HOMO and LUMO orbitals of the isolated molecule ($\text{S-C}_6\text{H}_4\text{-S}$) are indicated in (a) and (b).

ent from those of the DFT+NEGF-based calculations with atomic leads. The reason for this discrepancy is so far not clear; one possibility might be the artificial scattering at the jellium-Au interface.

D. Resonance mechanism

In order to show more clearly the mechanism of the resonance peak around the Fermi energy and the modification in transport properties caused by changing the contact Au-S distance, we show in Fig. 5 contour plots of transmission coefficient as functions of energy and $\Delta d_{\text{Au-S}}$ for the three S-anchored systems, (001)₂Au, (001)₀Au, and (001)₁Au. For the (001)₂Au system, when the Au-S dis-

tance is large ($\Delta d_{\text{Au-S}} > 1.0 \text{ \AA}$) there are three energies in the energy window which contribute to the electron transmission. Comparison with the level structure of the isolated molecule ($\text{S-C}_6\text{H}_4\text{-S}$) shows that these three energies correspond to the LUMO, highest energy occupied molecular orbital (HOMO), and HOMO-1 of the isolated molecule, respectively. As $\Delta d_{\text{Au-S}}$ decreases, the increasing molecule-lead coupling broadens these three levels. The two HOMO states shift gradually to lower energies as well. It is clear that the resonance peak around $\Delta d_{\text{Au-S}} = 0.2 \text{ \AA}$ in Fig. 4(a) originates from the (broadened) LUMO contribution.

For the (001)₀Au case and large Au-S distance ($\Delta d_{\text{Au-S}} > 1.4 \text{ \AA}$), the result is completely similar to that for the (001)₂Au system. This is a further indication that the two resonance peaks in Fig. 4(a) and 4(b) have the same character, as we already argued from the similarity $T(E)$ in Figs. 2(b) and 4(d). The role of the two additional Au atoms at the contacts is equivalent to that from increasing the surface-S distance. As $\Delta d_{\text{Au-S}}$ is decreased to smaller than 1.0 \AA the strong molecule-lead coupling changes significantly the local electronic structure, and we cannot distinguish the individual contribution from the molecular orbitals anymore. Finally, at $\Delta d_{\text{Au-S}} = 0.0 \text{ \AA}$ the transmission function becomes totally different from that for large $\Delta d_{\text{Au-S}}$, as shown in Fig. 2(a).

An interesting thing we should notice in Fig. 5(b) is that within the large range of $\Delta d_{\text{Au-S}} \sim 0-1 \text{ \AA}$ the equilibrium conductance is actually very insensitive to the Au-S distance. This indicates that the molecule-lead separation dependence of the equilibrium conductance can be quite complicated: it can be either very strong (for large $\Delta d_{\text{Au-S}}$) or very weak (for small $\Delta d_{\text{Au-S}}$).

For the (001)₁Au system, because of the strong coupling on the left side [see Fig. 1(c)] we cannot recognize the individual contributions from the molecular orbitals in Fig. 5(b) even for large $\Delta d_{\text{Au-S}}$. However, there is a similar LUMO-like contribution to the resonance peak in Fig. 4(c), and the equilibrium conductance is also insensitive to the Au-S distance for $\Delta d_{\text{Au-S}} \sim 0-1 \text{ \AA}$. This indicates that the total electron transmission is dominated by the weakly coupled contact.

E. I - V curve

The large resonance peak in the equilibrium transmission function around the Fermi energy suggests the possibility of negative differential conductance when a bias voltage is applied. We would like to show this explicitly. In order to avoid the large computational effort for the I - V curve of this system, we use a similar but slightly smaller system. The structure and equilibrium transmission function of the small system are shown in Fig. 6. As can be seen, the cross section of the lead here is smaller than that shown in Fig. 1(g) (i.e., the atoms in the surface layers in Fig. 1(g) are removed). It can be seen that its transmission function is somewhat different from that of the large system, but the feature of the large resonance peak around the Fermi energy is the same. The calculated I - V curve given in Fig. 6 shows clearly a large negative differential conductance around $V_b \sim 0.2-0.5 \text{ V}$.

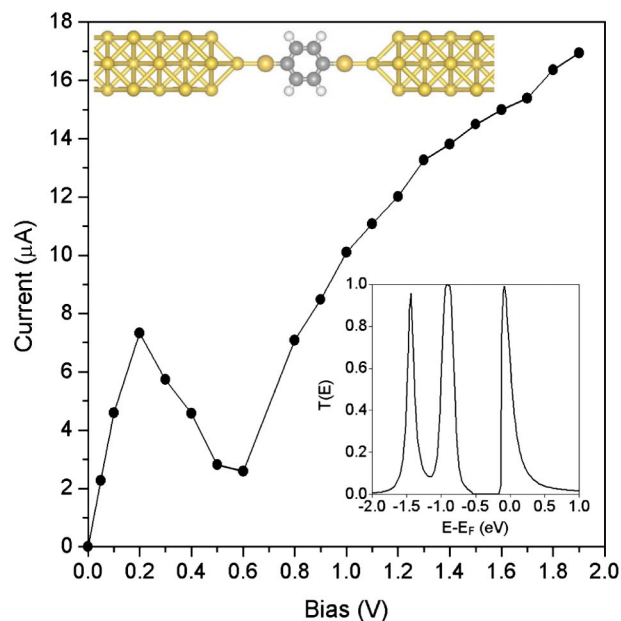


FIG. 6. I - V curve of the smaller (001)₂Au system shown in the upper inset, whose transmission function under zero bias is shown in the lower inset. Note that there is a large resonance peak in $T(E)$ around the Fermi energy which causes a large negative differential conductance in the I - V curve around $V_b = 0.2-0.5 \text{ V}$.

We would like to say that the use of the extremely thin lead may have some artificial effects on the result because in this case almost all the atoms in the leads are surface atoms and the screening is certainly not good, therefore, the result may not be quantitatively reliable. However, as we have shown above, the main features of the $T(E)$ function around the Fermi energy are still captured by using this very thin lead, so we can expect that the result here is still qualitatively meaningful.

IV. SUMMARY

By using a density functional theory calculation for molecular electronic structure and a Green function method for electron transport, we have calculated from first principles the molecular conductance of benzene sandwiched between two Au leads in different ways. In our calculation, the effects of contact atomic relaxation, two different lead orientations, and different anchoring atoms are fully considered. We focused on the effects of the change in atomic structure around the contacts, including the presence of an additional Au atom and changes in the molecule-lead separation, as an effort to simulate possible situations in break-junction experiments. Our findings are the following.

(1) The presence of an additional Au atom at each of the two contacts can increase the equilibrium conductance by one to two orders of magnitude *regardless* of the contact atomic structure or group-VI anchoring atom. The mechanism is the creation of a LUMO-like resonance peak around the Fermi energy, which also leads to negative differential conductance under applied bias.

(2) The presence of the additional Au atom at only one

contact will give only a minor increase in conductance because the electron transmission is then choked off by the other nontransparent contact.

(3) Because of the different molecule-lead coupling, the Au(001) and Au(111) leads will give different equilibrium conductances. This difference is significantly reduced by adding the additional Au atom at the contacts.

(4) The dependence of the equilibrium conductance on the molecule-lead separation is subtle: it can range from either very weak to very strong depending on the separation regimes.

ACKNOWLEDGMENT

This work was supported in part by the NSF (Grant No. DMR-0103003).

¹*An Introduction to Molecular Electronics*, edited by M. C. Petty and M. Bryce (Oxford University Press, New York, 1995).

²J. R. Heath and M. A. Ratner, *Phys. Today* **56**(5), 43 (2003).

³J. M. Tour, *Molecular Electronics* (World Scientific, Singapore, 2003).

⁴C. Joachim, J. K. Gimzewski, and A. Aviram, *Nature (London)* **408**, 541 (2000).

⁵A. Nitzan, *Annu. Rev. Phys. Chem.* **52**, 681 (2001).

⁶M. A. Reed, C. Zhou, C. J. Muller, T. P. Burgin, and J. M. Tour, *Science* **278**, 252 (1997).

⁷C. Kergueris, J. P. Bourgoin, S. Palacin, D. Esteve, C. Urbina, M. Magoga, and C. Joachim, *Phys. Rev. B* **59**, 12505 (1999).

⁸J. Reichert, R. Ochs, D. Beckmann, H. B. Weber, M. Mayor, and H. v. Löhneysen, *Phys. Rev. Lett.* **88**, 176804 (2002).

⁹A. F. Morpurgo, C. M. Marcus, and D. B. Robinson, *Appl. Phys. Lett.* **74**, 2084 (1999).

¹⁰H. Park, A. K. L. Lim, A. P. Alivisatos, J. Park, and P. L. McEuen, *Appl. Phys. Lett.* **75**, 301 (1999).

¹¹Y. V. Kervennic, H. S. J. Van der Zant, A. F. Morpurgo, L. Gurevich, and L. P. Kouwenhoven, *Appl. Phys. Lett.* **80**, 321 (2002).

¹²M. S. Fuhrer (private communication).

¹³R. H. M. Smit, Y. Noat, C. Untiedt, N. D. Lang, M. C. van Hemert, and J. M. van Ruitenbeek, *Nature (London)* **419**, 906 (2002).

¹⁴W. Kohn and L. J. Sham, *Phys. Rev.* **140**, A1133 (1965).

¹⁵R. G. Parr and W. Yang, *Density-Functional Theory of Atoms and Molecules* (Oxford University Press, New York, 1989i).

¹⁶N. D. Lang, *Phys. Rev. B* **52**, 5335 (1995).

¹⁷N. D. Lang and Ph. Avouris, *Phys. Rev. Lett.* **84**, 358 (2000).

¹⁸M. Di Ventra, S. T. Pantelides, and N. D. Lang, *Phys. Rev. Lett.* **84**, 979 (2000).

¹⁹N. D. Lang and Ph. Avouris, *Phys. Rev. B* **64**, 125323 (2001).

²⁰H. Haug and A.-P. Jauho, *Quantum Kinetics in Transport, Optics of Semiconductors* (Springer, Berlin, 1996).

²¹S. Datta, *Electronic Transport in Mesoscopic Systems* (Cambridge University Press, Cambridge, UK, 1995).

²²J. Taylor, H. Guo, and J. Wang, *Phys. Rev. B* **63**, 245407 (2001).

²³P. S. Damle, A. W. Ghosh, and S. Datta, *Phys. Rev. B* **64**, 201403 (2001).

²⁴Y. Xue, S. Datta, and M. A. Ratner, *Chem. Phys.* **281**, 151 (2002).

²⁵M. Brandbyge, J.-L. Mozos, P. Ordejón, J. Taylor, and K. Stokbro, *Phys. Rev. B* **65**, 165401 (2002).

²⁶E. Louis, J. A. Vergs, J. J. Palacios, A. J. Prez-Jimnez, and E. SanFabin, *Phys. Rev. B* **67**, 155321 (2003).

²⁷S.-H. Ke, H. U. Baranger, and W. Yang, *Phys. Rev. B* **70**, 085410 (2004).

²⁸Y. Xue, S. Datta, and M. A. Ratner, *J. Chem. Phys.* **115**, 4292 (2001).

²⁹Y. Xue and M. A. Ratner, *Phys. Rev. B* **68**, 115407 (2003).

³⁰Y. Xue and M. A. Ratner, *Phys. Rev. B* **68**, 115406 (2003).

³¹J. J. Palacios, A. J. Prez-Jimnez, E. Louis, E. SanFabin, and J. A. Vergs, *Phys. Rev. B* **66**, 035322 (2002).

³²J. J. Palacios, A. J. Prez-Jimnez, E. Louis, E. SanFabin, and J. A. Vergs, *Phys. Rev. Lett.* **90**, 106801 (2003).

³³S. K. Nielsen, M. Brandbyge, K. Hansen, K. Stokbro, J. M. van Ruitenbeek, and F. Besenbacher, *Phys. Rev. Lett.* **89**, 066804 (2002).

³⁴J. Taylor, M. Brandbyge, and K. Stokbro, *Phys. Rev. Lett.* **89**, 138301 (2002).

³⁵J. Taylor, M. Brandbyge, and K. Stokbro, *Phys. Rev. B* **68**, 121101 (2003).

³⁶C. Roland, B. Larade, J. Taylor, and H. Guo, *Phys. Rev. B* **65**, 041401 (2002).

³⁷H. Mehrez, A. Wlasenko, B. Larade, J. Taylor, P. Grtter, and H. Guo, *Phys. Rev. B* **65**, 195419 (2002).

³⁸C.-C. Kaun, B. Larade, H. Mehrez, J. Taylor, and H. Guo, *Phys. Rev. B* **65**, 205416 (2002).

³⁹C.-C. Kaun, B. Larade, and H. Guo, *Phys. Rev. B* **67**, 121411 (2003).

⁴⁰W. Lu, E. G. Wang, and H. Guo, *Phys. Rev. B* **68**, 075407 (2003).

⁴¹M. Di Ventra, N. D. Lang, and S. T. Pantelides, *Chem. Phys.* **281**, 189 (2002).

⁴²J. G. Rodrigo, A. García-Martín, J. J. Sáenz, and S. Vieira, *Phys. Rev. Lett.* **88**, 246801 (2002).

⁴³J. M. Soler, E. Artacho, J. D. Gale, A. Garcia, J. Junquera, P. Ordejón, and D. Sánchez-Portal, *J. Phys.: Condens. Matter* **14**, 2745 (2002).

⁴⁴J. P. Perdew, K. Burke, and M. Ernzerhof, *Phys. Rev. Lett.* **77**, 3865 (1996).

⁴⁵N. Troullier and J. L. Martins, *Phys. Rev. B* **43**, 1993 (1991).

⁴⁶In order to reduce the computational cost, we have tried to combine a DZP basis set for the molecule with a single zeta (SZ) basis set for the leads. We found a large difference from the result of the all-DZP calculation.

⁴⁷We have performed test calculations for a system consisting of a seven-carbon-atom chain sandwiched between two Al(001) leads adopting both *periodic boundary conditions* (by using SIESTA package) and a *cluster geometry* [by using a quantum chemistry package, NWChem (Ref. 48)]. We found large differences between the two results.

⁴⁸High Performance Computational Chemistry Group, NWChem, *A Computational Chemistry Package for Parallel Computers, Version 4.1* (Pacific Northwest National Laboratory, Richland, Washington, 2002).